The 2014 World Congress on
Advances in Civil, Environmental, and Materials Research (ACEM14)
Busan, Korea, August 24-28, 2014

Ferromagnetic and Dielectric Behavior of Bismuth Iron Oxide Nanoparticles under As-synthesized Conditions

Farzana Majid[1)], Saira Riaz[2)]and Shahzad Naseem[2)]

Centre of Excellence in Solid State Physics, University of the Punjab, Lahore 54590, Pakistan
[1)] saira.cssp@pu.edu.pk

ABSTRACT

Multiferroic materials are of particular interest due to the co-existence of ferromagnetic and ferroelectric properties. Among various multiferroics, bismuth iron oxide ($BiFeO_3$, BFO) is the only material that shows both ferroelectric and antiferromagnetic properties at room temperature. However, synthesis of phase pure BFO is difficult due to volatile nature of Bi_2O_3. In this work, bismuth iron oxide nanoparticles are synthesized using sol-gel technique. With change in synthesis conditions a transition from amorphous nature to crystalline behavior is observed. The crystalline nature of nanoparticles strongly affects the dielectric and magnetic properties. High dielectric constant of ~300 (frequency =1kHz) is obtained due to presence of less conducting grain boundaries. Ferromagnetic behavior, instead of antiferromagnetic bismuth iron oxide, arises due to suppression of spiral spin structure of bismuth iron oxide.

1. INTRODUCTION

During last few years, interest in multiferroic materials has risen due to simultaneous presence of two ferroic orders in the same phase i.e. ferromagnetic and ferroelectric ordering (Arora 2014). Such materials exhibit magnetoelectric coupling between electric and magnetic properties. Their magnetic properties can be controlled via application of electric field and electric polarization can be controlled via application of magnetic field (Arora 2014, Pavana 2013). Multiferroic materials have found wide applications in data storage devices, sensors, spintronic and optical devices (Arora 2014, Zhao 2013).

Various multiferroic materials have been reported to date including $Cr_3B_7O_{13}Cl$, $BiMnO_3$, $NdMn_2O_5$, $HoMnO_3$, $LuMnO_3$ etc. (Tripathy 2013). Among these materials, bismuth iron oxide is a potential candidate due to its high ferroelectric Curie temperature of 820˚C and antiferromagnetic Neel temperature of 370˚C (Tripathy 2013, Shah 2014(a)). Bismuth iron oxide ($BiFeO_3$, BFO) posses rhombohedral perovskite

---

[1)] Graduate Student
[2)] Professor

structure. Sterochemical activity connected with 6s2 lone pair of electron belonging to Bi3+ is responsible for multiferroic nature of BFO. This results in reduced crystal symmetry and consequently the ferroelectric properties. Magnetic properties in BFO is due to the presence of uncompensated spins at iron site. In BFO ferromagnetic coupling arises within the plane whereas, antiferromagnetic coupling arises between the spins of adjacent planes. Due to DM (Dzyaloshinsky-Moriya) interaction canted ferromagnetism arises (Mazumder 2006).

Despite the advantages of BFO, there are some complications associated with phase pure BFO including: 1) volatile nature of bismuth oxide that leads to presence of bismuth rich and/bismuth deficient phases; 2) antiferromagnetic nature 3) large leakage current.

Several methods have been reported to date for synthesis of phase pure BFO including hydrothermal method (Yan 2014), sol-gel auto-combustion method (Tripathy 2013), RF magnetron sputtering (Jian 2013), molecular beam epitaxy (Laughlin 2013), sol-gel method (Shah 2014(a,b)), pulsed laser deposition (Chang 2013).

For overcoming the difficulties associated with phase pure BFO, we here report the synthesis and characterization of bismuth iron oxide nanoparticles using sol-gel method.

2. EXPERIMENTAL DETAILS

For synthesis of bismuth iron oxide nanoparticles, bismuth nitrate and iron nitrate were used as precursors. Iron nitrate and bismuth nitrate were separately dissolved in ethylene glycol. Ethylene glycol, being a linearly structured molecule, helped in compensating for difference in hydrolysis rate of bismuth and iron. The two solutions were mixed together and heated on hot plate at 60˚C for several hours. The sol was then heat treated at 80˚C to obtain BFO nanoparticles (NPs). Two different methods were employed for synthesis of BFO NPs. The powders prepared were named as BFO-1 and BFO-2.

The NPs were characterized under as-prepared conditions. Structural characterizations were carried out using Bruker D8 Advance X-ray Diffractometer. For magnetic measurements Lakeshore's vibrating sample magnetometer was used. Dielectric properties of BFO NPs were carried out in parallel plate configuration using 6500B precision impedance analyzer.

3. RESULTS AND DISCUSSION

Fig. 1 shows XRD patterns for BFO NPs prepared using sol-gel method. BFO-1 show amorphous behavior (Fig. 1(a)). On the other hand, with change in synthesis conditions BFO-2 NPs show crystalline behavior. Diffraction peaks at 2θ˚=22.2˚, 39.9˚, 50.9˚, 52.2˚ and 60.5˚ corresponding to planes (012), (202), (211), (122) and (125) indicate the presence of $BiFeO_3$ phase. However, small diffraction peaks also indicate the presence of bismuth deficient $Bi_2Fe_4O_9$ phase (Fig. 1(b)).

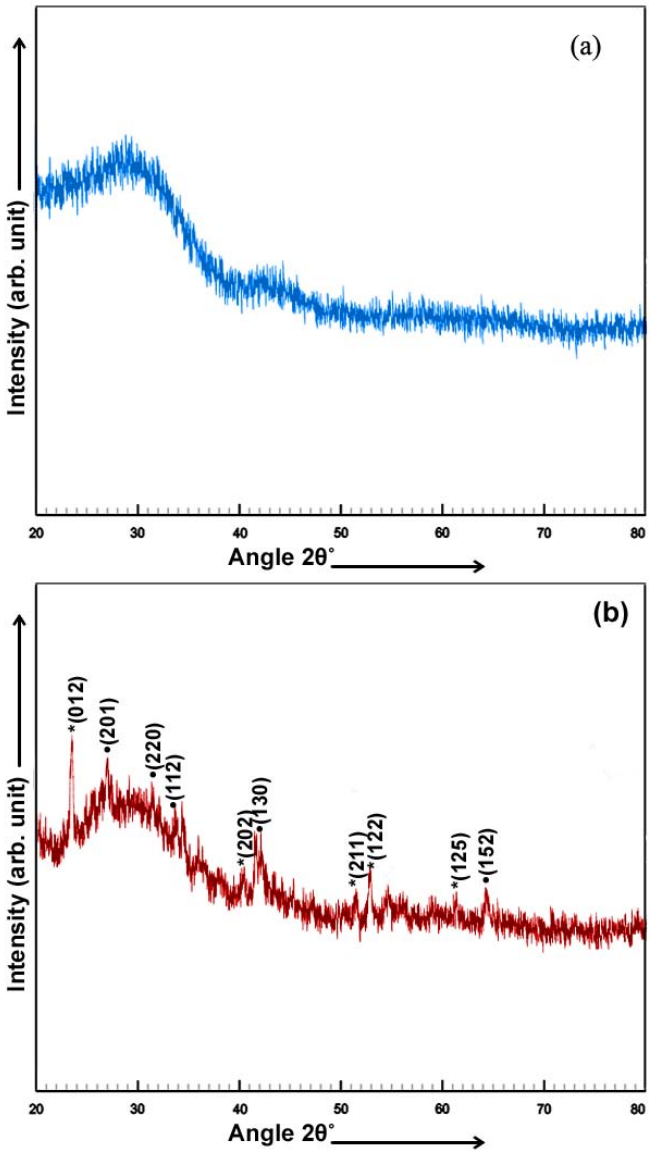

Fig. 1 XRD patterns for BFO NPs (a) BFO-1 (b) BFO-2

For studying the dielectric properties of bismuth iron oxide impedance analyzer was used in parallel plate configuration. The parallel capacitance and parallel resistance were measured and then using Eq. 1 and Eq. 2 the dielectric constant ε and dielectric loss (tangent loss tan δ) were calculated.

$$\varepsilon = \frac{C \times d}{\varepsilon_O \times A} \tag{1}$$

$$\tan\delta = \frac{1}{2\pi\varepsilon\varepsilon_O\rho} \tag{2}$$

Where, *C* is the capacitance, *d* is the thickness of the specimen, *A* the area of the device, ε_o is the permittivity of free space and ρ is the resistivity of NPs. Dielectric constant and tangent loss for BFO nanoparticles are plotted as a function of frequency

in Fig. 2. Dielectric constant and tangent loss decreases as the frequency of applied field increases and becomes constant at high frequencies. Decrease in dielectric constant at low frequencies can be explained on the basis of Maxwell-Wagner two layer model. According to this model, the specimen is composed to two layers: 1) grains 2) grain boundaries. Grains are more conducting as compared to grain boundaries. At low frequencies the role of grain boundaries dominates thus, resulting in high value of dielectric constant. At high frequencies the role of grains dominates that lead to reduction in dielectric constant.

The dielectric constant of BFO-2 nanoparticles (300 at f=1KHz) is high as compared to that of BFO-1 (150 at f=1kHz) with low value of tangent loss. The high value of dielectric constant is attributed to polycrystalline nature of BFO-2 (Fig. 1(b)). The polycrystalline nature of BFO-2 leads to increased number of grain boundaries that are less conducting thus resulting in high value of dielectric constant.

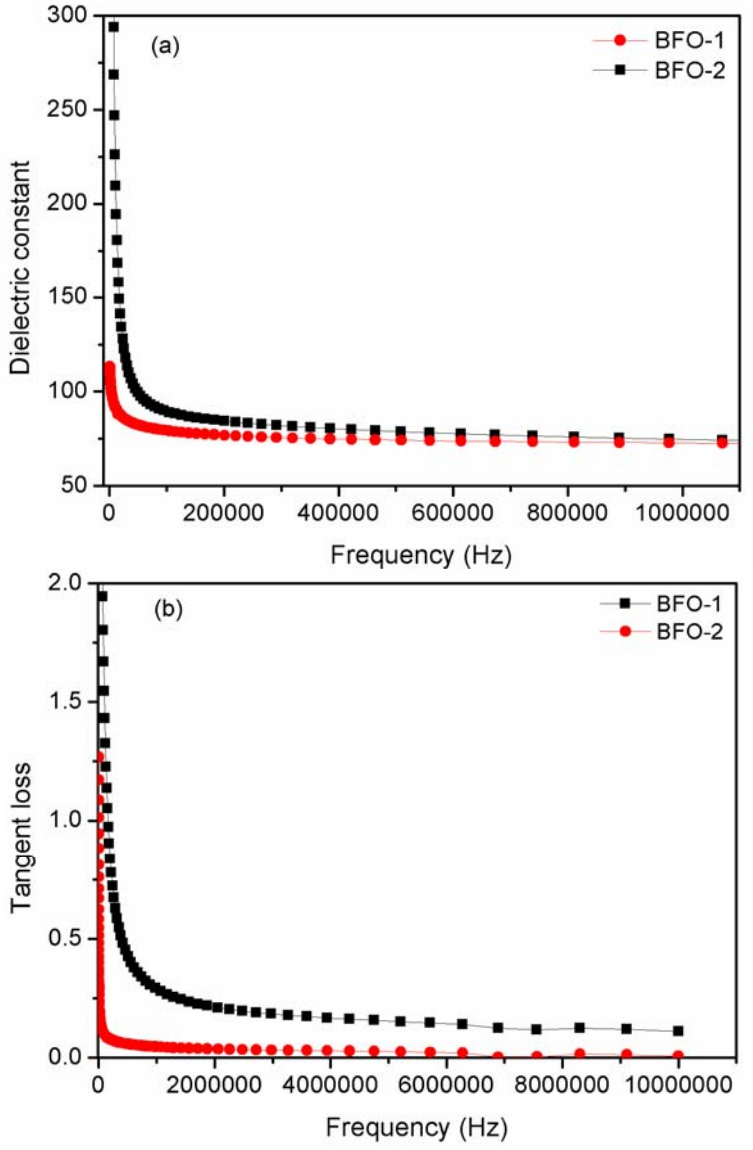

Fig. 2 (a) Dielectric constant (b) tangent loss as a function of dopant concentration

Fig. 3 show M-H curve for bismuth iron oxide nanoparticles prepared using sol-gel method. The particles show ferromagnetic behavior as opposed to antiferromagnetic nature of bulk BFO. The ferromagnetic behavior in BFO arises due to: 1) Suppression of spin structure. BFO has cycloidal spin arrangement of 620Å. So as the particle size fall below 620Å the helical spin structure is transformed to linear spin structure. This induces ferromagnetic behavior in otherwise antiferromagnetic BFO. 2) Presence of oxygen vacancies, 3) valence fluctuation of Fe^{3+} and Fe^{2+} cations.

BFO-2 nanoparticles show saturation magnetization of 1.75×10^{-3} emu. BFO-1 nanoparticles show saturation magnetization of $1.51.75\times10^{-3}$. Ferromagnetic behavior of BFO-1 and BFO-2 nanoparticles is indicative of the particle size below 62nm (cycloidal spin arrangement of BFO).

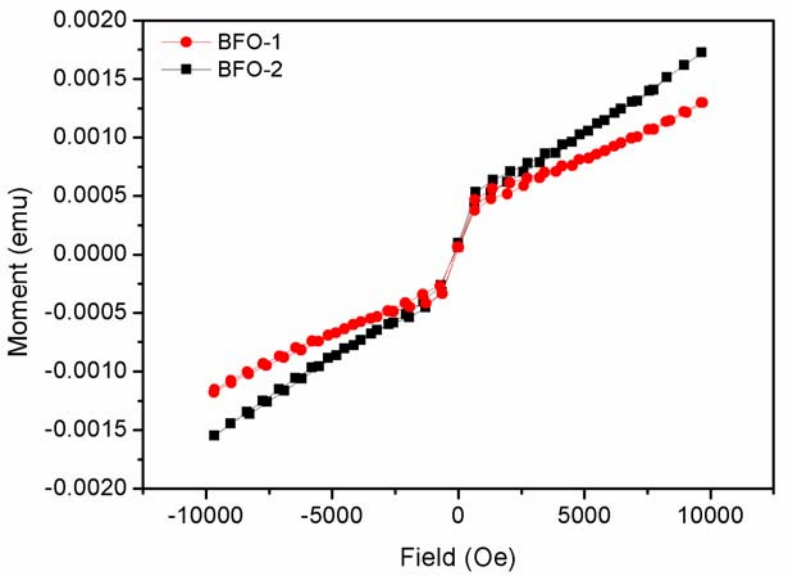

Fig. 3 M-H curves for BFO nanoparticles

4. CONCLUSIONS

Bismuth iron oxide nanoparticles are prepared using low cost, application oriented sol-gel method. Two different nanoparticles were prepared named as BFO-1 and BFO-2. BFO-2 nanoparticles show crystalline behavior while BFO-1 nanoparticles show amorphous behavior. High value of dielectric constant and low tangent loss is observed for BFO-2 nanoparticles due to their crystalline behavior. The nanoparticles show ferromagnetic behavior due to conversion of helical spin structure to linear spin structure.

REFERENCES

Arora, M., Chauhan, S., Sati, P.C. and Kumar, M. (2014), "Effect of non-magnetic ions substitution on structural, magnetic and optical properties of $BiFeO_3$ nanoparticles," *J. Supercond. Nov. Magn.*, DOI 10.1007/s10948-014-2521-4

Mocherla, P.S.V., Karthik, C., Ubic, R., Rao, M.S.R. and C. Sudakar, C. (2014), "Tunable bandgap in $BiFeO_3$ nanoparticles: The role of microstrain and oxygen defects," *Appl. Phys. Lett.*, **103**, 022910.

Zhao, J., Liu, S., Zhang, W., Liu, Z. and Liu, Z. (2013), "Structural and magnetic properties of Er-doped $BiFeO_3$ nanoparticles," *J. Nanopart. Res.,***15**, 1969

Tripathy, S.N., Mishra, B.G., Shirolkar, M.M., Sen, S., Das, S.R., Janes, D.B. and Pradhan, D.K. (2013), "Structural, microstructural and magneto-electric properties of single-phase $BiFeO_3$ nanoceramics prepared by auto-combustion method," Mater. Chem. Phys., **141**, 423-431

Mazumder, R., Ghosh, S., Mondal, P., Bhattacharya, D., S. Dasgupta, S., Das, N. and Sen, A. (2006), "Particle size dependence of magnetization and phase transition near T_N in multiferroic $BiFeO_3$," *J. Appl. Phys.*, **100**, 033908

Chang, H.W., Yuan, F.Y., Tien, S.H., Li, P.Y., Wang, C.R., Tu, C.S. and Jen, S.U. (2013), "High quality multiferroic $BiFeO_3$ films prepared by pulsed laser deposition on glass substrates at reduced temperatures," *J. Appl. Phys.*, **113**, 17D917

Jian, S.R., Chang, H.W., Tseng, Y.C., Chen, P.H. and Juang, J.Y. (2013), "Structural and nanomechanical properties of $BiFeO_3$ thin films deposited by radio frequency magnetron sputtering," *Nanoscale Res. Lett.*, **8**, 297

Laughlin, R.P., Currie, D.A., Guererro, R.C., Dedigama, A., Priyantha, W., Droopad, R., Theodoropoulou, N., Gao, P. and Pan, X. (2013), "Magnetic and structural properties of $BiFeO_3$ thin films grown epitaxially on $SrTiO_3$/Si substrates," *J. Appl. Phys.*, **113**, 17D919

Yan, D., Sun, C., Jian, J., Sun, Y., Wu, R. and Li, J. (2014), "Structure and phase transition of $BiFeO_3$ particles prepared by hydrothermal method and the verification of crystallization– dissolution–crystallization mechanism," *J. Mater. Sci.: Mater. Electron.*, **25**, 928–935.